Chapter 7
Droplet Collision

G. Brenn

Abstract We put together the state of knowledge on binary collisional interactions of droplets in a gaseous environment. Phenomena observed experimentally after drop collisions, such as coalescence, bouncing, reflexive separation and stretching separation, are discussed. Collisions of drops of the same liquid and of different – miscible or immiscible – liquids, as well as collisions of drops of equal and different size are addressed. Collisions of drops of immiscible liquids may lead to an unstable interaction which is not observed with drops of equal or miscible liquids. Regimes characterized by the various phenomena are depicted in nomograms of the Weber number and the non-dimensional impact parameter. The state-of-the-art in the simulation of binary droplet collisions is reviewed. Overall three different methods are represented in the literature on these simulations. We discuss models derived from numerical simulations and from experiments, which are presently in use for simulations of spray flows to account for the influence of collisional interactions of the spray droplets on the drop size spectrum of the spray.

Keywords Binary drop collisions · Bouncing · Coalescence · Collision model · Crossing separation · Gaseous environment · Immiscible liquids · Lattice-Boltzmann simulation · Miscible liquids · Navier–Stokes simulation · Reflexive separation · Satellite droplets · Spray flow simulation · SPH simulation · Stretching separation

Introduction

The present chapter puts together the state of knowledge about the collisional interaction of liquid droplets and gives an overview of the literature on experiments, as well as on simulation and modeling of binary liquid droplet collisions, both as an elementary phenomenon and also in the context of spray flows.

G. Brenn
Graz University of Technology, Institute of Fluid Mechanics and Heat Transfer, Graz, Austria
e-mail: brenn@fluidmech.tu-graz.ac.at

N. Ashgriz (ed.), *Handbook of Atomization and Sprays*,
DOI 10.1007/978-1-4419-7264-4_7,

We restrict this review to the case of binary collisions, i.e., to the processes caused by the impact of pairs of liquid droplets. Collisions of three or more droplets are much less investigated, since in spray flows they are much less probable than the binary case. Furthermore, the biggest part of this review will be devoted to droplets of Newtonian liquids. Investigations on collisions of non-Newtonian liquid droplets are very sparse in the literature, as will be discussed in more detail below. Also, since we are in the context of spray flows, we do not discuss collisions of droplets in another immiscible liquid host medium, but take the ambient medium as gaseous.

The importance of droplet collisions in dispersed gas-liquid two-phase flows with the liquid as the dispersed phase has been first recognized in the context of rainfall [1–5]. The first investigations on the effects of droplet collisions on liquid droplet ensembles emerged from the meteorological research on the evolution of clouds. The most important aspect of the collisional interaction of droplets in this context is the stability or instability of a collision, i.e., if the colliding drops merge and form a new stable drop with a volume equal to the sum of the volumes of the two original droplets, or if they separate and either maintain their original volumes or form droplets smaller than the original ones [6–25]. All research on droplet collisions concentrates on the description of the sizes of the droplets after the collision and does not put much emphasis on their velocities, since the velocity may be much more affected by aerodynamic forces from the gaseous host medium than by the collisional interaction itself. Furthermore the droplet size spectrum is the spray property of primary importance for the technological application of the sprays. Our present review therefore concentrates on this aspect.

Experimental Setups Used for Investigations of Drop Collisions

The droplet properties influencing droplet collisions are liquid physical properties as well as the size, velocity and trajectories of the droplets. From this we may conclude on the requirements to an experimental setup suitable for use in experimental studies of drop collisions. The equipment must include:

- Two droplet generators producing drops of controlled size and velocity
- Two reservoirs for supplying the test liquid(s)
- Manipulators allowing for control of the droplet trajectories and, in particular, the impact parameter
- A visualization system with illumination, either synchronized with the drop formation to produce standing pictures of the drops, or providing single short-time pulses for single-shot images
- A technique for measuring droplet diameter, either optical (e.g., phase-Doppler anemometry) or based on image processing

A setup with the essential components mentioned above, enabling experimental studies of droplet collisions, is shown in Fig. 7.1 [26]. In the literature we find

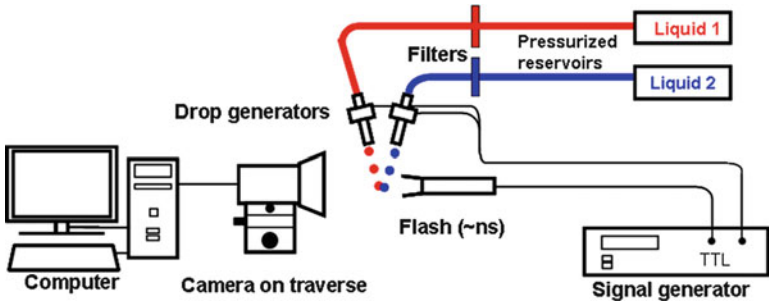

Fig. 7.1 Experimental setup for drop collision studies [26] (Reprinted from Colloids and Surfaces A – Physicochemical and Engineering Aspects. doi 10.1016/j.colsurfa.2009.12.011 (2009), Planchette, Lorenceau, Brenn, Liquid encapsulation by binary collisions of immiscible liquid drops, Copyright 2009, with permission from Elsevier)

a majority of works employing continuous-stream droplet generators for producing the colliding drops [27, 28]. Some researchers produced streams of electrically charged drops, intercepted by drops with different charge. The charged drops were deflected by a plate capacitor into a collector, while the drops with the different charge were removed from the streams and entered the collision region (Adam et al. [29]). The latter method had the advantage that the collision of pairs of single droplets could be realized and observed, without restriction of the largest allowable deformation due to neighboring drops in streams. Droplet generators used in the various studies worked on principles as reviewed in Chap. 10 of this handbook.

An important aspect in the collisional interaction of droplets is the influence of the ambient gaseous medium, which is mostly air. The influence of the gas pressure on the collisions has been subject of some studies (e.g., Qian and Law [30]), extending down to the case of vacuum [31, 32]. This kind of studies requires, of course, a vessel in which the droplet generators are placed, with the possibility to manipulate them from outside.

We now turn to a discussion of knowledge acquired by experiments on binary droplet collisions for various droplet liquids and sizes.

Phenomena in Binary Droplet Collisions

This part of our review summarizes the physical phenomena in binary liquid droplet collisions found in experimental investigations.

The collisional interaction of two liquid droplets, equal or unequal in size, is in general a complicated process, which does not allow for a theoretical description by analytical means. Typically, experimentalists provide insight into the regularities of the phenomena in such processes in the form of flow charts. The flow charts for binary droplet collisions known from the literature are nomograms depicting regimes characterized by certain mechanisms or phenomena occurring after the impact.

The independent variables in these charts emerge from the parameters influencing the collision process: the relative velocity U of the colliding droplets, the sizes d_s and d_l of the smaller and the larger droplet, the impact parameter b (i.e., the distance of closest approach of the centers of mass of the droplets, measured normal to the direction of the relative velocity, as sketched in Fig. 7.2), as well as the density ρ and dynamic viscosity μ of the droplet liquid and its surface tension σ against the ambient gas. This list of seven relevant parameters results in the following set of four characteristic numbers: the non-dimensional impact parameter $X = 2b/(d_s + d_l)$, the drop size ratio $\Delta = d_s/d_l$, the Ohnesorge number $\mathrm{Oh} = \mu/[\sigma\,(d_s + d_l)\,\rho/2]^{1/2}$, and the Weber number $\mathrm{We} = U^2(d_s + d_l)\rho/2\sigma$. Most flow charts represent the flow regimes for a given liquid system with known ρ, μ, and σ, and a given size of the colliding droplets, i.e., for constant Ohnesorge number. For simplicity, in the present section we restrict our discussion to colliding drops of equal (and constant) size d, so that the remaining set of parameters is represented by flow charts with the Weber number $\mathrm{We} = U^2 d\rho/\sigma$ as the abscissa variable and the non-dimensional impact parameter $X = b/d$ as the ordinate variable. A generic form of such a flow chart is shown in Fig. 7.3 [33]. This kind of a nomogram represents the droplet behavior for constant Ohnesorge number, i.e., with a given liquid and for constant drop size. A classification of the regimes of collision mechanisms specifies ranges of values of

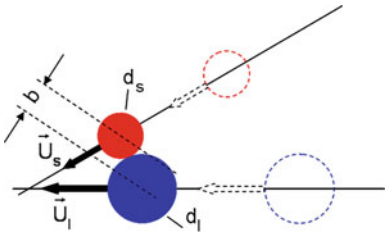

Fig. 7.2 Sketch of a collision of two drops of unequal size. The impact parameter b is measured normal to the direction of the relative velocity $\vec{U} = \vec{U}_s - \vec{U}_l$

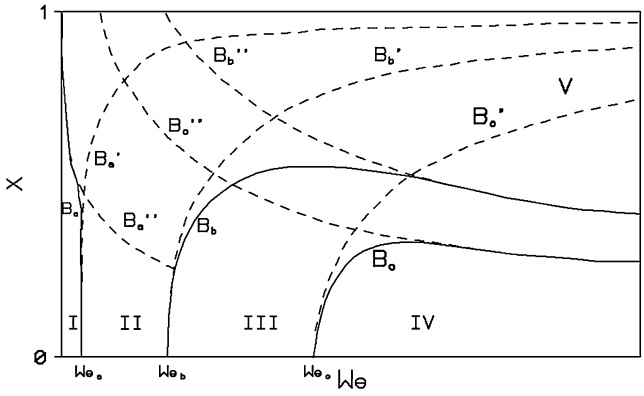

Fig. 7.3 Nomogram for binary collisions of equal-sized droplets for constant Ohnesorge number [33] (Reprinted with permission from [33], Copyright 1997 American Institute of Physics. Adapted from [34])

the Weber number We and the non-dimensional impact parameter X. Collisions with zero or reasonably small impact parameter are called *head-on collisions* or *near-head-on collisions*, respectively. For impacts with sufficiently large non-dimensional collision parameter, which are called *grazing collisions*, the system formed after the encounter is unstable and breaks up into two or more droplets.

We now discuss the phenomena observed after the collision of two droplets, associating typical values of We and X to them. The actual range of values of the characteristic numbers specifying the regimes discussed certainly depends on the pairing of the liquid and its ambient gas investigated, and on the drop size. The values of We and X we name are just typical values. Representative pictures of the processes are displayed in Fig. 7.4 [34]. We discuss the phenomena in the sense of increasing impact Weber number We. Starting at low values of the Weber number less than, say, 4, we find that the result of the drop collision is *coalescence* of the impacting droplets for all values of the impact parameter (Figs. 7.4a and b, regime I in Fig. 7.3). This means that, for this range of Weber numbers, colliding droplets always merge and form one larger drop with a volume equal to the sum of the two colliding droplets' volumes. Such a collision may be termed as stable in the sense that the deformation upon impact does not cause instability and disruption of the newly formed common surface of the liquid system. Collisions of this type have an influence on the drop size spectrum in a spray, since they make drops of given sizes disappear and produce larger drops.

With increasing value of the Weber number, a new phenomenon occurs, which is characterized by *bouncing* back of the drops after the impact (Fig. 7.4c, regime II in Fig. 7.3). This phenomenon occurs for all values of the impact parameter (Fig. 7.4d, regime II in Fig. 7.3). The reason for the occurrence of this mechanism is believed to be the inclusion of portions of the ambient gas between the droplets upon impact, which prevents the formation of a common surface of the colliding droplets. This inclusion of gas becomes possible due to the deformation of the drop surfaces upon approach of the droplets at a kinetic energy which is higher with this mechanism than in the collisions followed by coalescence in regime I. Numerical studies showed that it is the build-up of gas pressure between the two approaching droplets that may flatten the two sides of the droplets facing each other upon approach and cause bouncing. The reason for the pressure build-up is the gas flow resistance against drainage from the gap between the droplets [35]. This interpretation of the findings from the simulations is consistent with the experiments of Willis and Orme in a vacuum, where the build-up of a pressure is impossible and, consequently, bouncing was not observed [31]. It is interesting to note that, in cases of bouncing back of the colliding droplets, there is no mass transfer between the two droplets [36]. Due to obvious methodological difficulties, both in experiments and in numerical simulations, the physical reasons for the occurrence of this mechanism are not clarified in full detail yet. Bouncing of the droplets typically occurs in the range of Weber numbers between 4 and 10. It occurs for all values of the non-dimensional impact parameter X.

In collisions at Weber numbers greater than, say, 10, we observe that, for moderate non-dimensional impact parameter, the droplets merge and form one common drop (Figs. 7.4e and f, regime III in Fig. 7.3). The newly formed drop

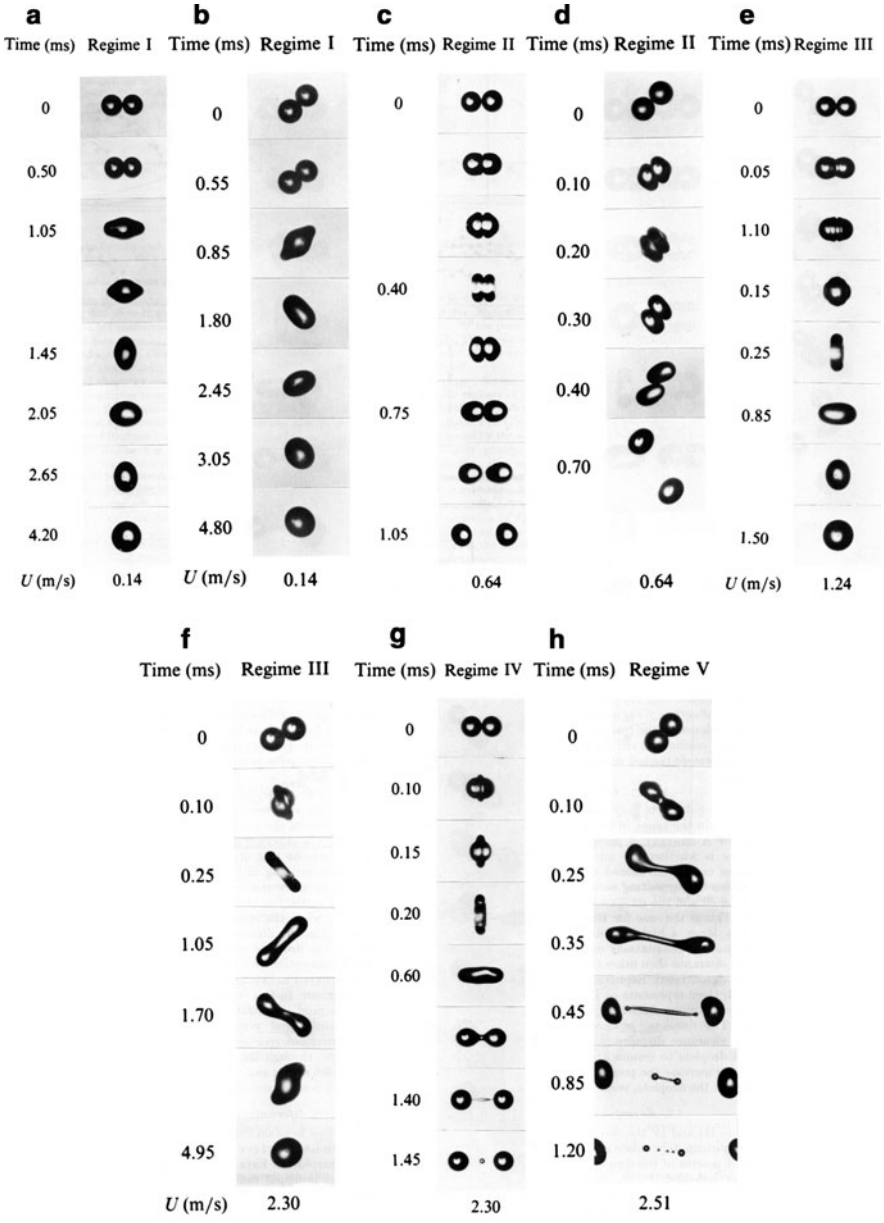

Fig. 7.4 Mechanisms in binary collisions of equal-sized droplets of the same liquid: (**a**) coalescence at low Weber numbers, head-on (regime I); (**b**) coalescence at low Weber numbers, grazing (regime I); (**c**) bouncing, head-on (regime II); (**d**) bouncing, grazing (regime II); (**e**) coalescence at higher Weber number, head-on (regime III); (**f**) coalescence at higher Weber number, grazing (regime III); (**g**) reflexive separation, head-on (regime IV); (**h**) stretching separation (regime V) [34]. Regimes referring to Fig. 7.3 ([34] Copyright, Cambridge Journals, reproduced with permission)

remains stable after the collision. The deformation-induced oscillations of the free surface are dampened, and the result is a spherical merged drop. The stability of this collision, however, is ensured only for sufficiently small non-dimensional impact parameter below, say, 0.5. The mechanism observed for parameters $X > 0.5$, which leads to break-up of the system formed by the collision, is called *stretching separation*, since it includes the formation of a liquid bridge or filament between the bulks of the colliding droplets, which is stretched due to the inertia-dominated motion of the droplets, eventually separates from the remaining portions of the original droplets, and breaks up into satellite droplets (Fig. 7.4h, regime V in Fig. 7.3) [37, 38]. If more than two droplets are formed by this process, all new droplets are smaller than the colliding droplets. The number of (satellite) droplets produced by the break-up of the liquid filament formed in stretching separation depends on the length of the liquid filament, i.e., on the Weber number and non-dimensional impact parameter. The onset value of the non-dimensional impact parameter for stretching separation typically decreases with increasing Weber number. The break-up of the filament into the satellite droplets follows a different mechanism for small and for large values of the impact parameter [38]. At small impact parameters, the mechanism is end-pinching, while it is a mixture of capillary wave growth and end-pinching for large impact parameters. The range of non-dimensional impact parameters leading to stretching separation is wide throughout the relevant range of collision Weber numbers, so that the occurrence of this mechanism is very probable for droplet collisions in sprays. This process influences a spray by making large drops disappear and producing droplets with small sizes, which is an influence on the drop size spectrum contrary to the effect of coalescence.

For still increasing value of the Weber number, a new phenomenon occurs for head-on and near-head-on collisions. A typical value of the onset Weber number for this phenomenon is 30. For these collisions, the stability of the liquid system formed by the encounter is lost, even at very low values of the non-dimensional impact parameter below, say, 0.3. In such collisions, the kinetic energy of the colliding drops is high enough to cause substantial deformations which lead to break-up of the liquid system, often into three droplets. This mechanism is called *reflexive separation* and is restricted to small values of the non-dimensional impact parameter (Fig. 7.4g, regime IV in Fig. 7.3). With increasing non-dimensional impact parameter, the dissipative influence of the increasing shear forces stabilizes the system, so that stable coalescence may occur. For sufficiently high non-dimensional impact parameter, however, stretching separation (regime V) is again observed.

The last mechanism to be discussed is characteristic of encounters of pairs of droplets with very high Weber number. This mechanism leads to large deformations of the drops upon impact, and to irregular break-up of the liquid system formed after the collision. It is called *droplet shattering*. The onset Weber number for this mechanism may be of the order of, say, 400, which is outside the range of Weber numbers investigated in most studies on droplet collisions. Exceptions are, e.g., the studies by Roth et al. [39], and by Willis and Orme [31, 32], where Weber numbers significantly greater than 2,000 are investigated. It is interesting to note that, in the vacuum environment of the experiments by Willis and Orme, shattering

collisions were not observed, despite the large Weber numbers of the collisions. This finding sheds light on the role of the gaseous environment in droplet shattering. Nonetheless, this mechanism is much less investigated than all the others, and, due to the irregular nature of the break-up after impact, its description in terms of drop sizes produced after the collision puts more difficulties than all the other mechanisms found in binary droplet collisions.

Equal and Unequal-Sized Droplets from the Same Liquid

Collisions of equal-sized droplets of the same liquid are the best investigated case in the present context. Regimes of the occurrence of the mechanisms discussed in section Phenomena in Binary Droplet Collisions are well known and explored for various liquids, such as water as well as simple alcohols and hydrocarbons up to the order of hexadecane.

The far more probable case in the collisional interaction of droplets in sprays, however, is the impact of droplets with different sizes. The literature on this case is much more sparse than for equal-sized droplets, but there exist results for certain values of the ratio $\Delta = d_s/d_l$ of the small to the large drop sizes. The most important kind of results are nomograms indicating the various regimes of the above discussed post-collisional mechanisms, which determine the outcome of the collision in terms of drop sizes and velocities. From these charts, mathematical descriptions of the regime boundaries are extracted, which may be used as criteria for the occurrence of the various mechanisms. Important examples for this kind of results are, e.g., the works by Adam et al. [29], Ashgriz and Poo [36], Jiang et al. [34], Qian and Law [30], and Estrade et al. [40, 41]. These authors investigate different liquids, such as water, *n*-alkanes and other hydrocarbons, and ethanol. Figures 7.5a–c show regimes as reported by Ashgriz and Poo [36], Qian and Law [30], and Estrade et al. [40], respectively.

Any mathematical representation of the regime boundaries must necessarily be limited to the liquids and drop sizes investigated, and provides information on the given liquid system in the given gaseous environment only. One model that accounts for the influence of the Ohnesorge number on the stability limit against stretching separation and on the formation of satellite droplets is due to Brenn and Kolobaric [38]. Here we present some equations describing limits between some regimes of different mechanisms. For their water droplets, Ashgriz and Poo [36] described the boundary between coalescence and reflexive separation as

$$We = \frac{3\Delta\left[7\left(1+\Delta^3\right)^{2/3} - 4\left(1+\Delta^2\right)\right]\left(1+\Delta^3\right)^2}{\left(\Delta^6\eta_1 + \eta_2\right)} \tag{7.1}$$

where $\eta_1 = 2(1-\xi)^2\,(1-\xi^2)^{1/2} - 1$, $\eta_2 = 2(\Delta-\xi)^2\,(\Delta^2-\xi^2)^{1/2} - \Delta^3$, with $\xi = 0.5X(1+\Delta)$. This equation was based on a formulation of the reflexive kinetic energy.

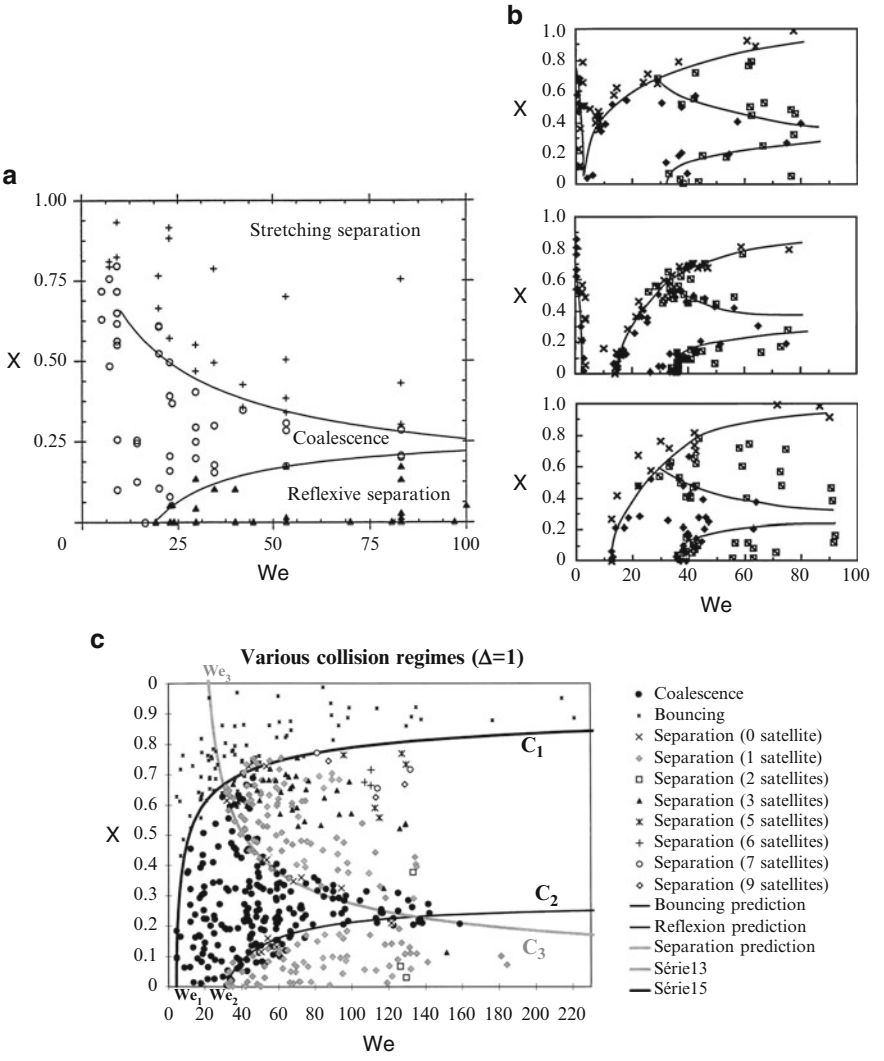

Fig. 7.5 Regimes of mechanisms determining the outcome from binary collisions of equal-sized droplets from various liquids: (**a**) regimes of coalescence, stretching separation and reflexive separation for water drops in air at atmospheric pressure [36]; (**b**) regimes of coalescence, bouncing, and reflexive separation for tetradecane droplets at the ambient nitrogen pressures of 0.6, 1, and 2.4 atm [30]; (**c**) regimes of coalescence, bouncing, reflexive separation and stretching separation for ethanol droplets in air at atmospheric pressure [40] ([30, 36] Copyright, Cambridge Journals, reproduced with permission. Reprinted from [40], Copyright 1999, with permission from Elsevier)

The authors postulate that this energy must be greater than 75% of the nominal surface energy of a nominal spherical combined mass formed after the collision for reflexive separation to occur. The equality in (7.1) represents the case where the 75% threshold is just reached. In an analogous way, Ashgriz and Poo [36]

obtain for the boundary between stable coalescence and stretching separation the criterion

$$We = \frac{4\left(1+\Delta^3\right)^2\left[3(1+\Delta)(1-X)\left(\Delta^3\phi_s+\phi_l\right)\right]^{1/2}}{\Delta^2\left[\left(1+\Delta^3\right)-(1-X^2)\left(\phi_s+\Delta^3\phi_l\right)\right]} \tag{7.2}$$

where

$$\phi_s = \begin{cases} 1-\dfrac{1}{4\Delta^3}(2\Delta-\tau)^2(\Delta+\tau) & \text{for } h>d_s/2 \\ \dfrac{\tau^2}{4\Delta^3}(3\Delta-\tau) & \text{for } h<d_s/2 \end{cases} \tag{7.3}$$

and

$$\phi_l = \begin{cases} 1-\dfrac{1}{4}(2-\tau)^2(1+\tau) & \text{for } h>d_l/2 \\ \dfrac{\tau^2}{4}(3-\tau) & \text{for } h<d_l/2 \end{cases} \tag{7.4}$$

with $\tau = (1 - X)(1 + \Delta)$ and $h = (d_l + d_s)(1 - X)/2$. This boundary compares favorably with experimental data and agrees better than the corresponding relations by Brazier-Smith et al. [42] and Arkhipov et al. [43, 44].

Equal-Sized Droplets from Different Miscible Liquids

Literature on the collision of droplets from different liquids is very sparse to date [45–48]. Gao et al. [45] investigated the collision of equal-sized droplets of water and ethanol, i.e., of two miscible liquids, in monodisperse streams produced by two piezoelectric drop generators. The drop sizes ranged between 400 and 600 μm. The authors provide a flow chart similar to that in Fig. 7.5a, where the Weber number is defined with the relative velocity of the colliding drops and the liquid properties of ethanol. The maximum value of the Weber number realized is 100. Upon contact between the droplet surfaces, the surface tension of the water decreases due to the presence of the ethanol. This leads to a Marangoni effect (called Unbalanced Surface Force [USF]) by Gao et al. [45]. At high non-dimensional impact parameters, this effect elongates the water drop and promotes its break-up into two portions, even at low Weber numbers. At intermediate non-dimensional impact parameters, the formation of a liquid finger is observed, which may pinch off and form a droplet if the impact Weber number is high enough. Finally, for head-on collisions, coalescence of the colliding drops or reflexive separation with formation of at least one satellite due to the "USF" are observed (Fig. 7.6). This field of research is still at its beginning to date.

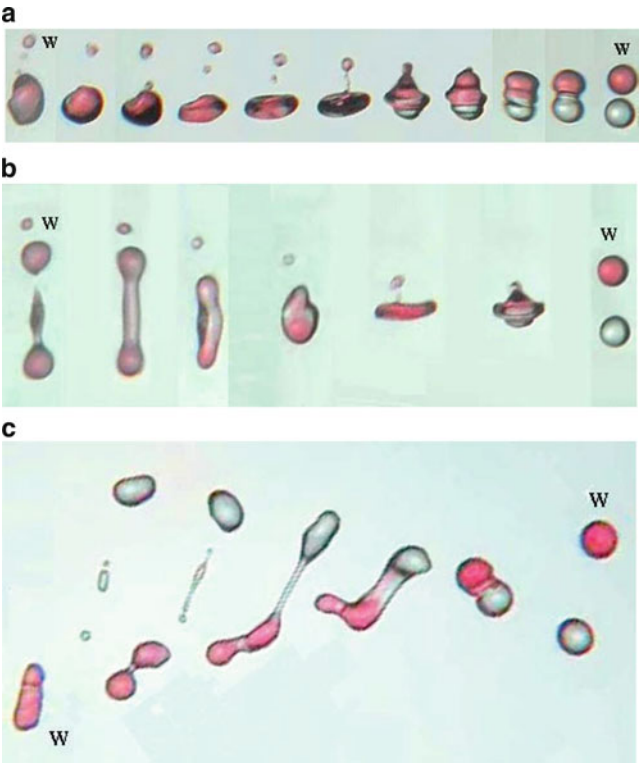

Fig. 7.6 Collisions of a water and an ethanol drop: (**a**) head-on collision with coalescence and separation of one satellite (We = 20, $X = 0$); (**b**) reflexive separation with formation of a small satellite due to Marangoni forces ($We = 38.5, X = 0.02$); (**c**) stretching separation with formation of three satellite droplets ($We = 82.3, X = 0.82$). Droplets move from right to left; the water droplet coming from above is marked with "w" [45] (With kind permission from Springer Science+Business Media: Experiments in Fluids [45], Plates 3, 5 & 6, Copyright Springer-Verlag 2005)

Equal-Sized Droplets from Different Immiscible Liquids

What was said about the state of knowledge on collisions of different miscible liquid drops applies to the case of immiscible liquids also. We find the work by Chen and Chen [49], who investigated the collision of equal-sized droplets of water and Diesel oil. The dynamic viscosities and surface tensions of the two liquids against air at the temperature of the experiments are different by a factor of 3.1 and 2.6, respectively. Drop sizes, produced with the same piezoelectric droplet generators as in Gao et al. [45], ranged between 700 and 800 μm. The result of an experimental survey of the outcome from the collisions for varying impact Weber number and non-dimensional impact parameter is a flow chart similar to that in Fig. 7.5a, where the Weber number is defined with the relative velocity of the colliding drops and the liquid properties of Diesel oil. The boundaries between the

regimes of bouncing, coalescence, reflexive separation, and stretching separation shown in the graph are sharp and convincing (Fig. 7.7). The maximum value of the Weber number realized is 100. What comes in as a new mechanism further to the well known ones with drops of equal or different, but miscible, liquids is a phenomenon called "overlaying action" by Chen and Chen [49]. By that mechanism, the Diesel oil encapsulates the water and forms a thin layer on top of the water drop. Such a process is observed in the head-on configuration ($X = 0$) from Weber numbers of 18.6 on. Three cases of head-on collisions with coalescence are shown in Fig. 7.8 [49]. In their paper, the authors do not undertake any modeling efforts.

One point should be made about the identification of a reflexive separation case in paper [49]. Reflexive separation is defined as an unstable post-collision mechanism that separates the droplets collided at near-head-on impact parameters. In this mechanism, the bulk masses of the colliding droplets remain on the sides of the symmetry plane from where they had approached (therefore "reflexive" separation). In the case shown in Fig. 7.9, however, which is identified as "single reflex separation" by Chen and Chen [49], the dyed drop changes its side from above (before collision) to below the symmetry plane (after collision), and the transparent drop moves vice versa. The actual mechanism therefore implies a mutual penetration of the liquid portions in the collided complex, which is not reflexive separation. This mechanism was called "crossing separation" by Planchette et al. [26] and by Planchette and Brenn [50], since the two liquid portions cross the trajectories of their respective collision partners.

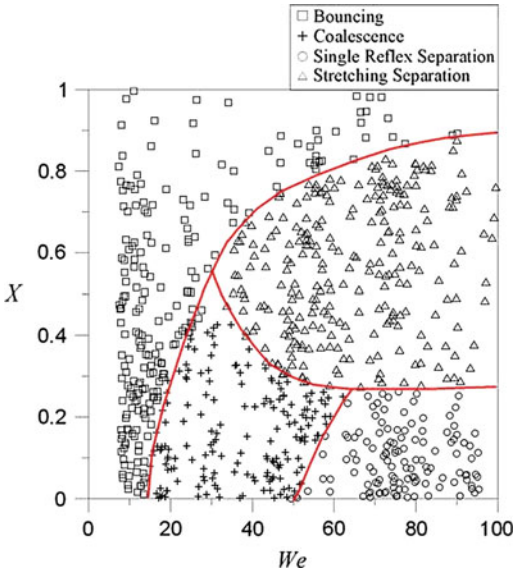

Fig. 7.7 Flow chart for the collision of equal-sized droplets of water and Diesel oil [49] (With kind permission from Springer Science+Business Media: Experiments in Fluids [49] Fig. 3, Copyright Springer-Verlag 2006)

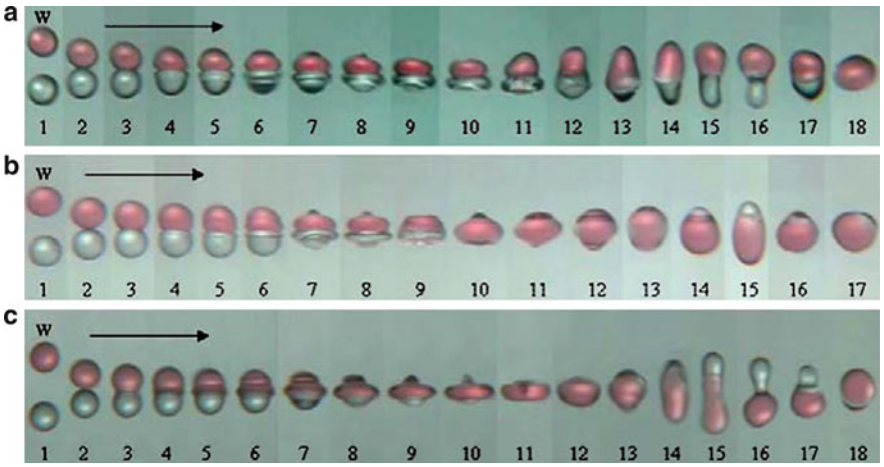

Fig. 7.8 Three cases of coalescence of droplets of water and diesel oil after head-on collisions: (**a**) $We = 18.6$, (**b**) $We = 28.7$, (**c**) $We = 45.3$. Droplets move from left to right; the red incoming water droplet is marked with "w" [49] (With kind permission from Springer Science+Business Media: Experiments in Fluids [49], Fig. 6, Copyright Springer-Verlag 2006)

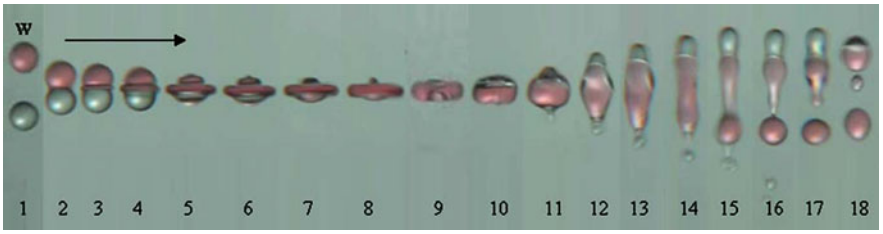

Fig. 7.9 Collision mechanism termed "single reflex separation" in Chen and Chen (2006) at $We = 95.3$, $X = 0$. Note that the colored liquid moves from above (before collision) to below the symmetry plane (after collision) [49]. The mechanism is, therefore, not reflexive (With kind permission from Springer Science+Business Media: Experiments in Fluids [49] Fig. 8, Copyright Springer-Verlag 2006)

Droplets of Non-Newtonian Liquids

A prerequisite for experimental investigations with colliding droplets is the controlled production of the colliding droplets, where the control concerns both the size and the velocity of the droplets. For controlled droplet production in the experiments, researchers employ droplet generators producing jets that are forced to break up into droplets of equal size due to a vibrational excitation. This process works properly – if satellite droplet formation can be suppressed – with Newtonian liquids, even of appreciable dynamic viscosities. Any non-Newtonian flow behavior of the liquids, in particular elasticity, however, makes a difference in this respect. Even small concentrations of, e.g., polymeric substances in Newtonian

solvents lead to the build-up of elastic stresses upon elongational and/or shearing motion of the liquid, which delays the jet break-up and makes the controlled formation of monodisperse streams of droplets very difficult. With strain-hardening elastic liquids, the formation of a beads-on-a-string structure is observed in this process, and the pinch-off of the liquid filaments (strings) between the droplets cannot be controlled by the vibrational excitation. The resulting drop size, which is influenced by the retraction of portions of the filaments into the adjacent droplets, is therefore far less controlled than with Newtonian liquids. This practical experimental difficulty may cause the lack of experiments on viscoelastic liquid droplet collisions in the literature [51].

However, the situation is different for shear-thinning, inelastic liquids. Motzigemba et al. [52] report about experiments and numerical simulations on collisions of droplets with shear-thinning flow behavior. The liquid was an aqueous solution of carboxymethylcellulose (CMC). Head-on collisions of droplets of this liquid with the Weber number of 766, comparable to collisions of droplets of an aqueous glycerol solution with a dynamic viscosity of 100 mPa s (We = 657), showed that the non-Newtonian droplets experienced deformations after the impact that were larger by a factor of ≈ 2 than the Newtonian counterparts. Experiments at different Weber numbers all showed the same trend. A numerical simulation accounting for the non-Newtonian flow behavior of the CMC solution by a modified power law reproduced the maximum deformation of the droplets upon impact well, but showed some delay in the retraction at the later stages of deformation. The simulations also exhibited some shortcomings due to the entrapment of air between the colliding droplets, which was not observed in any of the experiments.

Another kind of non-Newtonian liquid droplets investigated for its collisional behavior are suspension droplets. In these heterogeneous fluids, the mass fraction of the solid matter dispersed in the liquid, the bulk density of the solid, and the solid particle size spectrum come into play as additional parameters influencing the dynamic behavior of the droplets in binary collisions. The group around Schulte and Fritsching reported about experiments on binary suspension droplet collisions. The solid particles consisted of china clay (kaolin), glass and polyamide. Typical ranges of the solid particle sizes were between 4 and 10 μm and between 10 and 15 μm, while the drop sizes were varied between 20 and 500 μm. One finding from the experiments was that the number of satellite droplets formed after grazing collisions decreases with increasing size of the solid particles suspended in the liquid [53]. We may state that this field of research in drop collisions is also still at its beginning.

Simulations of Droplet Collisions

The value of simulations of droplet collisions lies in the potential to analyze the temporal and spatial evolutions of the surface of the liquid system, and of contributions to the energy budget of the system from surface and kinetic energies during

the collision, and in the potential to vary quickly physical parameters of the collision in parameter studies. In particular, properties of the liquid systems, such as velocity fields, which are very difficult to measure, may be quantified by the simulations and related to the respective mechanism, such as, e.g., bouncing, where the velocity field in the liquid may play an essential role.

We report about the computational techniques used for simulations of the elementary process of a binary droplet collision and important results. We find overall three techniques used for the simulations.

Solving the Equations of Change of Continuum Mechanics

The most straight forward approach may be seen in solving the equations of change of continuum mechanics describing the collision process [54–62]. These are the equations of change for mass and momentum, together with the material law quantifying the flow behavior of the liquid. For incompressible Newtonian liquids, the equations to be solved are the Navier–Stokes equations. This approach implies the necessity to describe the dynamics of a liquid system with free surface under the action of inertial, viscous, and capillary forces. For this task, the location and shape of the free surface of the system must be tracked such that the capillary forces may be derived from the curvature of the interface. The biggest challenge is the simulation of the pinch-off of liquid portions from the liquid system, as it takes place, e.g., in stretching separation when the remainders of the original drops pinch off from the liquid filament stretched in the grazing collision. This leads to the need for a high spatial resolution of the numerical grid, and/or spatial adaptivity to avoid excessively large numbers of grid cells. For tracking the interface, most simulations use the Volume-of-Fluid (VoF) or Level-Set methods. Simulations based on these methods are able to reproduce the collision parameters for the onset of reflexive separation and stretching separation found in experiments as functions of the collision Weber number reasonably well. Grid sizes are typically up to 1.6 million cells. Figure 7.10 shows the surface shapes of droplets in a head-on and a grazing collision of two water droplets in air, as simulated by solving the Navier–Stokes equations [54]. The Reynolds and Weber numbers of the collision are 2,500 and 38, respectively, which corresponds approximately to a relative velocity at the impact of $U = 1.1$ m/s and a drop size $d = 2.3$ mm. In the grazing collision, the non-dimensional impact parameter $X = 0.55$.

Lattice-Boltzmann Simulations

One alternative to solving the equations of change of continuum mechanics for simulating droplet collisions is the lattice-Boltzmann approach [63–67]. This technique describes the liquid dynamics on the basis of the dynamics of particle motion, which represents the liquid dynamic behavior and is governed by the lattice-Boltzmann

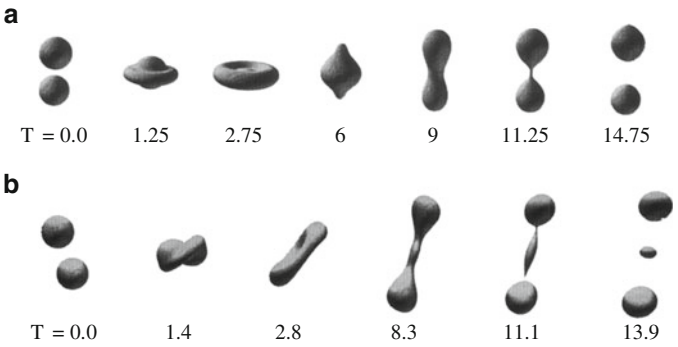

Fig. 7.10 Shapes of droplets produced by an unstable (**a**) head-on and (**b**) grazing collision of two equal-sized water droplets in air, at $Re = 2{,}500$ and $We = 38$, as simulated by solving the Navier–Stokes equations. In (**b**), the non-dimensional impact parameter $X = 0.55$; the non-dimensional time is defined as $T = t\ U/d$ [54] (Reprinted from [54], Copyright 1995, with permission from Elsevier)

equation. The equation allows for discrete directions of motion of the particles only. Various approaches with different numbers of directions of motion are established in the literature. The macroscopic properties of the liquid are derived from probability density functions of particle properties transported in the simulations. Simulations known from the literature use typical grids with 1.4 million cells. Interface shapes simulated for, e.g., grazing binary droplet collisions agree remarkably well with experiments. Also, the non-dimensional impact parameter at the onset of stretching separation as a function of the Weber number is represented well by these simulations. One drawback of this method, however, remains the fact that the physical parameters of the droplet liquid (dynamic viscosity, density, surface tension) represented in these simulations are far from the real values in the experiments. Insofar, the method implies some empiricism which remains unresolved. Figure 7.11 shows the shapes of droplets formed by the grazing collision of two equal-sized droplets at $Re = 100$ and $We = 106$, as observed in an experiment with propanol-2 droplets in air, and simulated with the lattice-Boltzmann method. The data correspond approximately to a relative velocity at the impact of 9.3 m/s and a drop size of 33 μm [63]. The non-dimensional impact parameter $X = 0.484$. The droplets in the experiment were markedly larger than the size corresponding to the characteristic parameters of the simulation.

Simulations Using Smoothed-Particle Hydrodynamics

The smoothed-particle hydrodynamics (SPH) method is an empirical alternative to the two above discussed methods, since it is grid-free and the results are, therefore, independent of a prescribed coordinate system and numerical grid resolution. It is

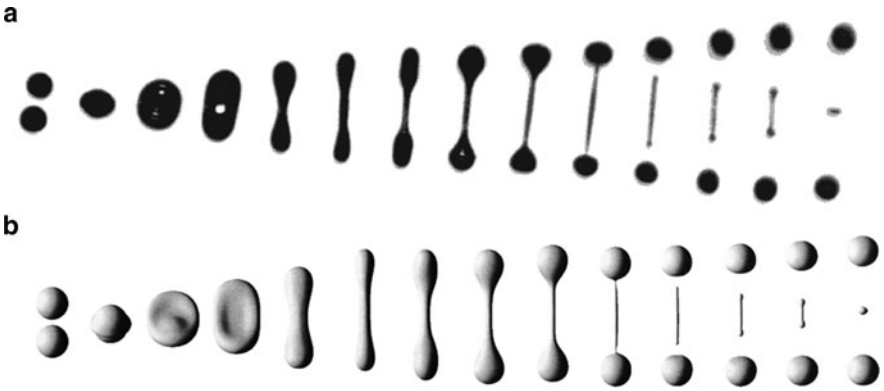

Fig. 7.11 Shapes of droplets produced by an unstable grazing collision of two equal-sized propanol-2 droplets in air at $Re = 100$ and $We = 106$ – (**a**) experiment, (**b**) lattice-Boltzmann simulation. The non-dimensional impact parameter $X = 0.484$ [63] (Reprinted with kind permission from Dr. Markus Schelkle, Immenstaad (Germany) 2010)

therefore suitable for simulating (discontinuous) free-surface flows with large deformations. The method is used to solve the equations of change of continuum mechanics, including the thermal energy equation. A further equation to be included in the formalism is the Lagrangian equation of motion of the particles. The formal discretization of the equations of change is obtained through the use of an interpolating kernel function that provides the estimate of the field variables at a set of particles suitably chosen to represent the fluid elements. The method describes the mean values of macroscopic parameters of a flowing fluid as convolution integrals of the parameter with the kernel function. This integral is approximated as a sum over neighboring particles [68]. The simulation referenced here, however, treats a collision of two-dimensional droplets, i.e., it simulates the collision of two circular cylinders. In the paper by Meleán and Sigalotti [68], only qualitative comparisons between the simulations and experimental results are drawn, without illustrations by diagrams or pictures. This method may be considered as being at its beginning and of limited use for simulating the complicated three-dimensional processes at hand. Figure 7.12 displays the evolution of the shapes of the "drop" cross sections in time, as simulated for a stable grazing collision of two circular cylinders at $X = 0.5$, $Re \approx 31$ and $We \approx 2$.

The overall conclusion from this brief survey is that the state-of-the-art in simulating binary droplet collisions may be considered as well advanced and capable of revealing details of the flow fields in the droplets and representing the sizes of droplets produced, which are difficult to access in the experiment. Nonetheless, the difficulty in correctly representing the process of pinch-off of portions from the liquid system, i.e., the simulation of the decrease of a liquid bridge diameter down to zero, remains unsolved in all methods known from the literature.

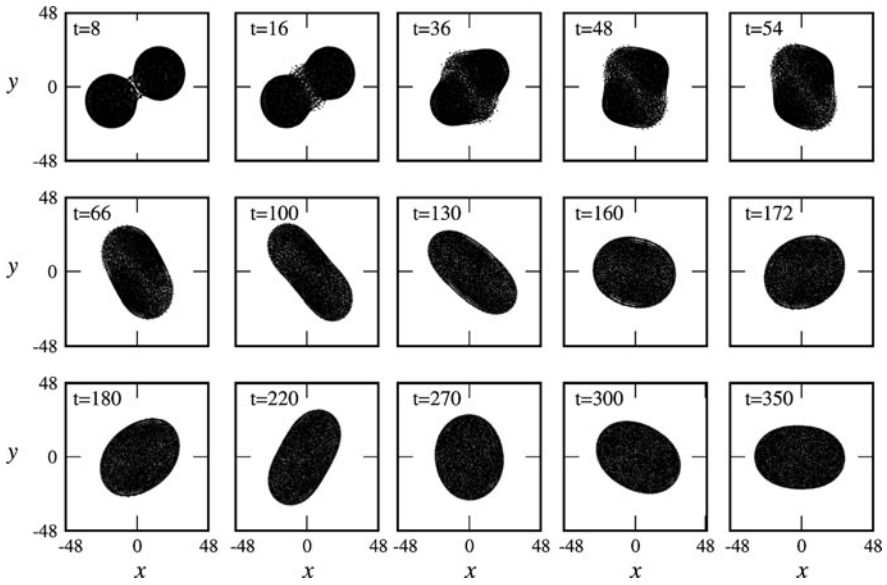

Fig. 7.12 Shapes of droplets produced by a stable grazing collision of two equal-sized two-dimensional droplets at $Re \approx 31$ and $We \approx 2$. The non-dimensional impact parameter $X = 0.5$. The non-dimensional time t is the ratio of the dimensional time to the scale $\mu d/2\sigma$ [68] (Reprinted from [68], Copyright 2005, with permission from Elsevier)

Modeling Binary Droplet Collisions in Spray Simulations

Modeling of the complicated phenomena in binary droplet collisions occurring in spray flows is difficult due to the variety of potential outcomes from a collision [69–71]. The first necessity is to predict the stability against stretching or reflexive separation. Then, for unstable drop collisions, the resulting drop sizes need to be predicted. All predictions should follow from algebraic models without the need to solve additional transport equations in the spray flow code to account for the collisions. Needless to say that it is impossible to simulate the full detail of the processes in droplet collisions, as done in the simulations discussed in section Simulations of Droplet Collisions, in the course of a spray flow simulation [72–82].

The task of modeling binary droplet collisions in Euler–Lagrangian simulations of spray flows was first taken up by O'Rourke and coworkers. Their model in [83] first estimates the coalescence efficiency, which is the probability that coalescence occurs after the collision, once it has taken place:

$$e_{\text{coal}} = \min\left\{1.0, \left[\frac{2.4f(\Delta)}{\text{We}}\right]\right\} \tag{7.5}$$

where the function $f(\Delta)$ reads

$$f(\Delta) = \Delta^{-3} - 2.4\Delta^{-2} + \frac{2.7}{\Delta} \tag{7.6}$$

and Δ is the ratio of sizes of the smaller to the larger droplet. In the model, the non-dimensional impact parameter X is chosen as a random number from the interval between 0 and 1. Collisions with $X<\sqrt{e_{\text{coal}}}$ are taken as stable and assumed to lead to coalescence. Collisions with $X>\sqrt{e_{\text{coal}}}$ are taken as unstable grazing collisions. In the coalescence case, the size and velocity of the new formed drops are computed from algebraic equations of conservation of volume and momentum. In the grazing case, the drops are assumed to conserve their sizes, and the new velocities are computed from an algebraic momentum equation. This means that the formation of satellite droplets by grazing collisions is ignored in this model, and the mechanism of bouncing is not included. Nonetheless, the "O'Rourke model" is termed the standard approach to calculating collisions in Lagrangian spray simulations even today [84].

The model by O'Rourke and coworkers has been extended and improved by several researchers. Schmidt and Rutland [84] developed a new algorithm for drop collision simulations, which is based on the no-time-counter method. The computational cost of this method is proportional to the number of computational particles, while the original algorithm of O'Rourke is proportional to its square. Through this improvement, spray simulations accounting for drop collisions may run several orders of magnitude faster (and slightly more accurate) than the original O'Rourke method. Zhang et al. [85] presented a method for reducing the mesh dependency of the simulation results, which they based on a model called the "cross mesh collision" (CMC) model. The model was implemented into the KIVA code. With three given meshes of different spatial resolution, the original O'Rourke model yielded Sauter Mean Radii of the droplets varying between 35 and 65 μm, while for the same conditions the new CMC model yielded variations only between 30 and 37 μm. Stralin et al. [86] added models based on similar criteria as laid out below to account for the post-collision behavior of the droplets and the formation of small fragments.

Some approaches exist today that identify and account for the various collision mechanisms in Euler–Lagrangian spray simulations. These models achieve best agreement with experimental data on interacting irregular streams of unequal-sized droplets and interacting sprays. Munnannur and Reitz [87] developed such a model, which accounts for the mechanisms bouncing, coalescence, stretching separation, reflexive separation, and separation at high Weber numbers. The regimes are identified according to the Weber number and the non-dimensional impact parameter: for *bouncing*, the criterion

$$We < \frac{\Delta\left(1+\Delta^2\right)(4\Theta' - 12)}{\chi_1[\cos(\arcsin X)]^2} \tag{7.7}$$

developed by Estrade et al. [40] is used, where the shape factor $\Theta' = 3.351$. The function χ_1 depends on the sizes of the smaller and larger colliding drops, and on the impact parameter, and reads

$$\chi_1 = 1 - 0.25(2-\tau)^2(1+\tau) \quad \text{for } (d_s + d_l)(1-X) > d_l \tag{7.8}$$

and

$$\chi_1 = 0.25\tau^2(3-\tau) \quad \text{for } (d_s + d_l)(1-X) \leq d_l. \tag{7.9}$$

Here, $\tau = (1-X)(1+\Delta)$, and d_s and d_l are the sizes of the smaller and the larger colliding drops, respectively. The bouncing of the droplets leaves the drop sizes unchanged. For *coalescence* of the colliding drops, the efficiency is quantified according to (7.5), and the velocity and size of the drop after merging are computed according to the simple volume and momentum balances described above.

Stretching separation is treated accounting for the break-up behavior of the liquid filament formed between the smaller and larger colliding drop bulk masses. The liquid volume in the filament is modeled according to a separation volume coefficient C_{vs} defined as

$$C_{vs} = \frac{E_{strtch} - E_{surten} - E_{dissip}}{E_{strtch} + E_{surten} + E_{dissip}} \tag{7.10}$$

where the energies involved are E_{strtch} – the total effective stretching kinetic energy, E_{surten} – the surface energy in the region of interaction of the two droplets, and E_{dissip} – the viscous dissipation in the interaction region. The first two energies are estimated according to Ashgriz and Poo [36]; the third energy E_{dissip} is assumed to be 30% of the total initial kinetic energy of the droplets for a stretching separation process. The filament formed between the bulbous ends of the liquid system in stretching separation is assumed to be uniform in radius. The length δ and radius r of the filament are time-dependent and inter-related, so that the volume remains constant. The derivative w.r.t. time of an energy balance for the filament results in a differential equation for the radius of the filament as a function of time, which accounts for viscous dissipation. The solution of a simplified version of this differential equation, together with a relation between the time to break-up of the filament and its radius at the instant of break-up, yields a nonlinear algebraic equation for the radius of the filament at break-up, which involves two model constants. The values of these constants are tuned to yield best agreement with experiments. Since the mechanism responsible for the break-up of the filament is assumed to be the Rayleigh mechanism, a simple equation relates the radius of the satellite droplets formed to the radius of the filament at break-up. The dominance of this mechanism in satellite droplet formation, however, depends on the ratio of two time scales: the inverse stretching rate of the filament and the capillary time scale $t_\sigma = \left(\rho r_0^3/\sigma\right)^{1/2}$. This time scale ratio, termed T, is therefore given as $T = t_\sigma \dot{\delta}/\delta$.

For sufficiently small T, the outcome from a stretching separation process is assumed to be the two remaining portions from the smaller and the larger colliding droplets plus one single satellite droplet, since, according to the results of Brenn et al. [33], this is the most probable case for all Weber numbers between 47 and 350. A threshold value of T is found to be 2: for $T \leq 2$, the single satellite is formed. For $T > 2$, the filament is stretched, and the number of satellites is calculated from volume conservation of the ligaments, assuming uniform size of the satellites.

The occurrence of *reflexive separation* is detected using the criterion developed by Ashgriz and Poo [36], which is formulated in (7.1) above. When reflexive separation occurs, again the time scale ratio T is checked against a threshold value, which is 3 for this mechanism. For $T \leq 3$, the ligament formed in reflexive separation contracts into one single "satellite"; the size of this satellite is the volume-equivalent size of the merged collided droplets. For $T > 3$, the ligament is stretched and undergoes break-up. The number and size of the satellites is computed following the same procedure as for stretching separation, but with a different initial length scale r_0 [87]. As an alternative to this model, the one developed by Post and Abraham [88] provides a comparable degree of detail.

Earlier, Georjon and Reitz [89] developed an additional "shattering collision" model that describes the break-up of droplets after collisions with high Weber numbers. As high Weber numbers in the sense of that model, the authors considered values above 100. There is some contradiction of this modelling approach to results, e.g., by Estrade et al. [40] and Brenn et al. [90], who showed that stretching separation with satellite droplet formation, as described in the model of Munnannur and Reitz [87] above, may take place at Weber numbers as high as 130 and 350, respectively. A model for shattering collisions as presented in paper [89] by Georjon and Reitz, is certainly a valuable extension to the drop collision models available in the literature, especially for the simulation of spray flows with high relative drop velocities where shattering collisions are highly probable.

References

1. P. R. Brazier-Smith, S. G. Jennings, J. Latham: Accelerated rates of rainfall, Nature 232, 112–113 (1971).
2. D. M. Whelpdale, R. List: The coalescence process in raindrop growth, J. Geophys. Res. 76, 2836–2856 (1971).
3. R. List, J. R. Gillespie: Evolution of raindrop spectra with collision-induced breakup, J. Atmos. Sci. 33, 2007–2013 (1976).
4. S. G. Bradley, C.D Stow: On the production of satellite droplets during collisions between water drops falling in still air, J. Atmos. Sci. 36, 494–500 (1979).
5. T. B. Low, R. List: Collision, coalescence and breakup of raindrops. Part I: Experimentally established coalescence efficiencies and fragment size distributions in breakup, J. Atmos. Sci. 39, 1591–1606 (1982).
6. D. J. Ryley, B. N. Bennett-Cowell: The collision behaviour of steam-borne water drops, Int. J. Mech. Sci. 9, 817–833 (1967).

7. P. R. Brazier-Smith, S. G. Jennings, J. Latham: An investigation of the behaviour of drops and drop-pairs subjected to strong electrical forces, Proc. R. Soc. Lond. A 325, 363–376 (1971).
8. A. M. Podvysotsky, A. A. Shraiber: Coalescence and break-up of drops in two-phase flows, Int. J. Multiphase Flow 10, 195–209 (1984).
9. N. Ashgriz, P. Givi: Binary collision dynamics of fuel droplets, Heat Fluid Flow 8, 205–210 (1987).
10. N. Ashgriz, P. Givi: Coalescence efficiencies of fuel droplets in binary collisions, Int. Commun. Heat Mass Transfer 16, 11–20 (1989).
11. G. Brenn, A. Frohn: Collision and merging of two equal droplets of propanol, Exp. Fluids 7, 441–446 (1989).
12. G. Brenn, A. Frohn: Collision and coalescence of droplets of various liquids, J. Aerosol Sci. 20, 1027–1030 (1989).
13. A. Menchaca-Rocha, A. Cuevas, M. Chapa, M. Silva: Rotating-liquid-drop model limit tested on macroscopic drops, Phys. Rev. E 47, 1433–1436 (1993).
14. C. K. Law: Dynamics of droplet collision, Proceedings of the IUTAM Symposium Mechanics and Combustion of Droplets and Sprays, Tainan, Taiwan, pp. 99–118 (1994).
15. J. Qian, C. K. Law: Effects of liquid and ambient gas properties on droplet collision, AIAA paper 94–0681 (1994).
16. A. Menchaca-Rocha, F. Huidobro, A. Martinez-Davalos, K. Michaelian, A. Perez, V. Rodriguez, N. Cârjan: Coalescence and fragmentation of colliding mercury drops, J. Fluid Mech. 346, 291–318 (1997).
17. M. Orme: Experiments on droplet collisions, bounce, coalescence and disruption, Prog. Energy Combust. Sci. 23, 65–79 (1997).
18. C. C. Hung, J. K. Martin: Collisional behavior of hydrocarbon droplets, Proceedings of the 10th Annual Conference Liquid Atomization and Spray Systems (ILASS Americas), Ottawa, Ontario (CDN) 1997, pp. 62–66 (1997).
19. J. Eggers, J. R. Lister, H. A. Stone: Coalescence of liquid drops, J. Fluid Mech. 401, 293–310 (1999).
20. L. Duchemin, J. Eggers, C. Josserand: Inviscid coalescence of drops, J. Fluid Mech. 487, 167–178 (2003).
21. F. Mashayek, N. Ashgriz, W. J. Minkowycz, B. Shotorban: Coalescence collision of liquid drops, Int. J. Heat Mass Transfer 46, 77–89 (2003).
22. G. A. Bach, D. L. Koch, A. Gopinath: Coalescence and bouncing of small aerosol droplets, J. Fluid Mech. 518, 157–185 (2004).
23. P. Duru, D. L. Koch, C. Cohen: Experimental study of turbulence-induced coalescence in aerosols, Int. J. Multiphase Flow 33, 987–1005 (2007).
24. C. Gotaas, P. Havelka, H. A. Jakobsen, H. F. Svendsen, M. Hase, N. Roth, B. Weigand: Effect of viscosity on droplet-droplet collision outcome: experimental study and numerical comparison, Phys. Fluids 19, paper 102106 (2007).
25. F.-C. Wang, J.-T. Feng, Y.-P. Zhao: The head-on colliding process of binary liquid droplets at low velocity: high-speed photography experiments and modelling, J. Colloid Interface Sci. 326, 196–200 (2008).
26. C. Planchette, E. Lorenceau, G. Brenn: Liquid encapsulation by binary collisions of immiscible liquid drops, Colloids Surf. A: Physicochem. Eng. Aspects 365, 89–94 (2010).
27. R. W. Park, E. J., Crosby: A device for producing controlled collisions between pairs of drops, Chem. Eng. Sci. 20, 39–45 (1965).
28. J. M. Schneider, N. R. Lindblad, C. D. Hendricks: An apparatus to study the collision and coalescence of liquid aerosols, J. Colloid Sci. 20, 610–616 (1965).
29. J. R. Adam, N. R. Lindblad, C. D. Hendricks: The collision, coalescence, and disruption of water droplets, J. Appl. Phys. 39, 5173–5180 (1968).
30. J. Qian, C. K. Law: Regimes of coalescence and separation in droplet collision, J. Fluid Mech. 331, 59–80 (1997).

31. K. D. Willis, M. Orme: Experiments on the dynamics of droplet collisions in a vacuum, Exp. Fluids 29, 347–358 (2000).
32. K. Willis, M. Orme: Binary droplet collisions in a vacuum environment: an experimental investigation of the role of viscosity, Exp. Fluids 34, 28–41 (2003).
33. G. Brenn, St. Kalenderski, I. Ivanov: Investigation of the stochastic collisions of drops produced by Rayleigh breakup of two laminar liquid jets, Phys. Fluids 9, 349–364 (1997).
34. Y. J. Jiang, A. Umemura, C. K. Law: An experimental investigation on the collision behaviour of hydrocarbon droplets, J. Fluid Mech. 234, 171–190 (1992).
35. Y. Pan, K. Suga: Numerical simulation of binary liquid droplet collision, Phys. Fluids 17, paper 082105 (2005).
36. N. Ashgriz, J. Y. Poo: Coalescence and separation in binary collisions of liquid drops, J. Fluid Mech. 221, 183–204 (1990).
37. A. Y. Tong, Z. Y. Wang: Relaxation dynamics of a free elongated liquid ligament, Phys. Fluids 19, paper 092101 (2007).
38. G. Brenn, V. Kolobaric: Satellite droplet formation by unstable binary drop collisions, Phys. Fluids 18, paper 087101 (2006).
39. N. Roth, M. Rieber, A. Frohn: High energy head-on collision of droplets, Proceedings of the Annual Conference Liquid Atomization and Spray Systems (ILASS Europe), Toulouse, July 1999.
40. J.-P. Estrade, H. Carentz, G. Lavergne, Y. Biscos: Experimental investigation of dynamic binary collision of ethanol droplets – a model for droplet coalescence and bouncing, Int. J. Heat Fluid Flow 20, 486–491 (1999).
41. J.-P. Estrade, P. Berthoumieu, G. Lavergne, Y. Biscos: Experimental investigation of dynamic binary collision of various liquids, Proceedings of the 8th International Symposium Flow Visualization, Sorrento, Italy, September 1998.
42. P. R. Brazier-Smith, S. G. Jennings, J. Latham: The interaction of falling water drops: coalescence, Proc. R. Soc. Lond. A 326, 393–408 (1972).
43. V. A. Arkhipov, G. S. Ratanov, V. F. Trofimov: Experimental investigation of the interaction of colliding droplets, J. Appl. Mech. Tech. Phys. 2, 73–77 (1978).
44. V. A. Arkhipov, I. M. Vasenin, V. F. Trofimov: Stability of colliding drops of ideal liquid, J. Appl. Mech. Tech. Phys. 3, 95–98 (1983).
45. T.-C. Gao, R.-H. Chen, J.-Y. Pu, T.-H. Lin: Collision between an ethanol drop and a water drop, Exp. Fluids 38, 731–738 (2005).
46. R. H. Chen: Diesel-diesel and diesel-ethanol drop collisions, Appl. Thermal Eng. 27, 604–610 (2007).
47. C. H. Wang, W. G. Hung, S. Y. Fu, W. C. Huang, C. K. Law: On the burning and microexplosion of collision-generated two-component droplets: miscible fuels, Combust. Flame 134, 289–300 (2003).
48. S. F. Simpson, J. R. Kincaid, F. J. Holler: Microdroplet mixing for rapid reaction kinetics with Raman spectrometric detection, Anal. Chem. 55, 1420–1422 (1983).
49. R. H. Chen, C. T. Chen: Collision between immiscible drops with large surface tension difference: diesel oil and water, Exp. Fluids 41, 453–461 (2006).
50. C. Planchette, G. Brenn: Liquid encapsulation by binary collisions of immiscible liquid drops, Proceedings of the 11th International Conference Liquid Atomization Spray Systems (ICLASS 2009), Vail, abstract ICLASS2009–243.
51. P. T. Yue, J. J. Feng, C. Liu, J. Shen: Diffuse-interface simulations of drop coalescence and retraction in viscoelastic fluids, J. Non-Newtonian Fluid Mech. 129, 163–176 (2005).
52. M. Motzigemba, N. Roth, D. Bothe, H.-J. Warnecke, J. Prüss, K. Wielage, B. Weigand: The effect of non-Newtonian flow behaviour on binary droplet collisions: vof-simulation and experimental analysis, Proceedings of the 18th Annual Conference Liquid Atomization Spray Systems (ILASS Europe), Zaragoza, Spain, pp. 559–564 (2002).

53. O. Kurt, U. Fritsching, G. Schulte: Secondary droplet formation during binary suspension droplet collision, Atomization Sprays 19, 457–472 (2009).
54. M. Rieber, A. Frohn: Three-dimensional Navier-Stokes simulation of binary collisions between droplets of equal size, J. Aerosol Sci. 26(Suppl. 1), S929–S930 (1995).
55. M. R. Nobari, Y.-J. Jan, G. Tryggvason: Head-on collision of drops – a numerical investigation, Phys. Fluids 8, 29–42 (1996).
56. M. R. H. Nobari, G. Tryggvason: Numerical simulations of three-dimensional drop collisions, AIAA J. 34, 750–755 (1996).
57. M. Rieber, A. Frohn: Navier-Stokes simulation of droplet collision dynamics, Proceedings of the 7th International Symposium CFD, Beijing, China, pp. 520–525 (1997).
58. M. Z. Dai, D. P. Schmidt: Numerical simulation of head-on droplet collision: effect of viscosity on maximum deformation, Phys. Fluids 17, paper 041701 (2005).
59. S. Tanguy, A. Berlemont: Application of a level set method for simulation of droplet collisions, Int. J. Multiphase Flow 31, 1015–1035 (2005).
60. S. P. Decent, G. Sharpe, A. J. Shaw, P. M. Suckling: The formation of a liquid bridge during the coalescence of drops, Int. J. Multiphase Flow 32, 717–738 (2006).
61. X. Jiang, A. J. James: Numerical simulation of the head-on collision of two equal-sized drops with van der Waals forces, J. Eng. Math. 59, 99–121 (2007).
61. N. Nikolopoulos, K.-S. Nikas, G. Bergeles: A numerical investigation of central binary collision of droplets, Comp. Fluids 38, 1191–1202 (2009).
63. M. Schelkle, M. Rieber, A. Frohn: Numerische Simulation von Tropfenkollisionen, Spektrum der Wissenschaft 1, 72–79 (1999).
64. T. Inamuro, S. Tajima, F. Ogino: Lattice Boltzmann simulation of droplet collision dynamics, Int. J. Heat Mass Transfer 47, 4649–4657 (2004).
65. B. Sakakibara, T. Inamuro: Lattice Boltzmann simulation of collision dynamics of two unequal-size droplets, Int. J. Heat Mass Transfer 51, 3207–3216 (2008).
66. M. Schelkle: Lattice-Boltzmann-Verfahren zur Simulation dreidimensionaler Zweiphasenströmungen mit freien Oberflächen, Ph.D. thesis University of Stuttgart, Shaker, Aachen, Germany (1997).
67. M. Schelkle, A. Frohn: Three-dimensional lattice Boltzmann simulations of binary collisions between equal droplets, J. Aerosol Sci. 26(Suppl. 1), S145–S146 (1995).
68. Y. Meleán, L. Di G. Sigalotti: Coalescence of colliding van der Waals liquid drops, Int. J. Heat Mass Transfer 48, 4041–4061 (2005).
69. J. K. Dukowicz: A particle-fluid numerical model for liquid sprays, J. Comp. Phys. 35, 229–253 (1980).
70. G. H. Ko, H. S. Ryou: Modeling of droplet collision-induced breakup process, Int. J. Multiphase Flow 31, 723–738 (2005).
71. L. E. Kollár, M. Farzaneh, A. R. Karev: Modeling droplet collision and coalescence in an icing wind tunnel and the influence of these processes on droplet size distribution, Int. J. Multiphase Flow 31, 69–92 (2005).
72. A. Kitron T. Elperin, A. Tamir: Stochastic modelling of the effects of liquid droplet collisions in impinging streams absorbers and combustors, Int. J. Multiphase Flow 17, 247–265 (1991).
73. M. Gavaises, A. Theodorakakos, G. Bergeles, G. Brenn: Evaluation of the effect of droplet colllisions on spray mixing, Proc. Inst. Mech. Eng. 210, 465–475 (1996).
74. P. Villedieu, J. Hylkema: Une méthode particulaire aléatoire reposant sur une équation cinétique pour la simulation numérique des sprays denses de gouttelettes liquides, C.R. Acad. Sci. Paris vol. 325, Série I, 323–328 (1997).
75. J. Dohmann: Dispersion and coagulation of droplets in intersecting sprays, Chem. Eng. Technol. 21, 341–345 (1998).
76. R. Kaesemann, H. Fahlenkamp: The meaning of droplet-droplet interaction for the wet fluegas cleaning process, Chem. Eng. Technol. 25, 739–742 (2002).
77. D. P. Schmidt, C. J. Rutland: Reducing grid dependency in droplet collision modelling, J. Eng. Gas Turbines Power 126, 227–233 (2004).

78. G. H. Ko, H. S. Ryou: Droplet collision processes in an inter-spray impingement system, J. Aerosol Sci. 36, 1300–1321 (2005).
79. C. Bautsch, H. Fahlenkamp: Detailed simulation of wet flue-gas-desulphurisation scrubbers with CFD, Proceedings of the International Conference on Liquid Atomization Spray Systems (ICLASS 2006), Kyoto, Japan, paper ICLASS06–238.
80. S. Hou, D. P. Schmidt: Adaptive collision meshing and satellite droplet formation in spray simulations, Int. J. Multiphase Flow 32, 935–956 (2006).
81. L. E. Kollár, M. Farzaneh: Modeling the evolution of droplet size distribution in two-phase flows, Int. J. Multiphase Flow 33, 1255–1270 (2007).
82. S. Hou, D. P. Schmidt: Interaction mechanisms between closely spaced sprays, SAE Technical Paper 2008-01-0946 (2008).
83. P. J. O'Rourke, F. V. Bracco: Modelling of drop interactions in thick sprays and a comparison with experiments, Proc. Inst. Mech. Eng. 9, 101–116 (1980).
84. D. P. Schmidt, C. J. Rutland: A new droplet collision algorithm. J. Comp. Phys. 164, 62–80 (2000).
85. H.-Y. Zhang, Y.-S. Zhang, B. Xu, C.-I. Mo: Extension of O'Rourke droplet collision model: application to diesel spray of single-hole injector, SAE Technical Paper 2006-01-3335 (2006).
86. P. Stralin, F. Wahlin, N. Nordin, H.-E. Angström: A Lagrangian collision model applied to an impinging spray nozzle, SAE Technical Paper 2006-01-3331 (2006).
87. A. Munnannur, R. D. Reitz: A new predictive model for fragmenting and non-fragmenting binary droplet collisions, Int. J. Multiphase Flow 33, 873–896 (2007).
88. S. L. Post, J. Abraham: Modeling the outcome of drop-drop collisions in Diesel sprays, Int. J. Multiphase Flow 28, 997–1019 (2002).
89. T. L. Georjon, R. D. Reitz: A drop-shattering collision model for multidimensional spray computations, Atomization Sprays 9, 231–254 (1999).
90. G. Brenn, D. Valkovska, K. D. Danov: The formation of satellite droplets by unstable binary drop collisions, Phys. Fluids 13, 2463–2477 (2001).